Wet-Ra: Monitoring Diapers Wetness with Wireless Signals

MENG XUE, Wuhan University, China
YANJIAO CHEN, Wuhan University, China
XUELUAN GONG, Wuhan University, China
JIAN ZHANG, Wuhan University, China
CHUNKAI FAN, Wuhan University, China

Diaper wetness monitoring is essential in various situations (e.g., babies and patients) to guarantee hygiene and avoid embarrassment. Existing diaper wetness monitoring methods include indicator lines, special sensors, and RFID, which require modifications on every diaper piece and cannot be easily checked under visual occlusions (e.g., trousers). In this paper, we introduce *Wet-Ra*, a contactless, ubiquitous, and user-friendly diaper wetness monitoring system based on RF signals. To extract informative features for wetness detection from RF signals, we construct Continuous-Radio-Snapshot and build corresponding signal representations that capture the distinct patterns of diapers of different wetness levels. We refine the signal representation by eliminating multi-path interference from the environment and mitigating the smearing effect with wavelet multisynchrosqueezing transform. To expand the usability of *Wet-Ra*, we build a transferable model that yields robust detection results in diversified environments and for new users. We conduct extensive experiments to evaluate *Wet-Ra* with 47 volunteers in 7 different rooms with three off-the-shelf diaper brands. Experiment results confirm that *Wet-Ra* can accurately identify diaper wetness in the real environment.

CCS Concepts: • **Human-centered computing → Ubiquitous and mobile computing**; **Ubiquitous and mobile computing systems and tools**.

Additional Key Words and Phrases: Diaper, Wetness monitoring, Wireless Sensing, Contactless Sensing

ACM Reference Format:
Meng Xue, Yanjiao Chen, Xueluan Gong, Jian Zhang, and Chunkai Fan. 2022. *Wet-Ra*: Monitoring Diapers Wetness with Wireless Signals. *Proc. ACM Interact. Mob. Wearable Ubiquitous Technol.* 6, 2, Article 84 (June 2022), 26 pages. https://doi.org/10.1145/3534599

1 INTRODUCTION

Diapers are worn by infants and adults of advanced age or with certain conditions (e.g., Alzheimer's, polyuria, and bed-bound patients). Wet diapers need to be changed to avoid discomfort, bacterial infection, and incontinence-associated dermatitis (IAD). Therefore, continuous monitoring of diaper wetness is of essential assistance to parents and caregivers for timely change of diapers.

Many commercial diapers on the market, e.g, Depend [2], Tena [11], Elderjoy [5], and Lifree [8], use wetness indicators that will change color when the diaper is wet. However, the caregiver must regularly check the diaper to directly see the indicator, which is inconvenient and does not give timely feedback. To realize automatic

Authors' addresses: Meng Xue, xuemeng@whu.edu.cn, Wuhan University, China; Yanjiao Chen, chenyanjiao@whu.edu.cn, Wuhan University, China; Xueluan Gong, xueluangong@whu.edu.cn, Wuhan University, China; Jian Zhang, jzhang@whu.edu.cn, Wuhan University, China; Chunkai Fan, fanchunkai@whu.edu.cn, Wuhan University, China.

2474-9567/2022/6-ART84 $15.00
https://doi.org/10.1145/3534599

Table 1. A comparison of diaper wetness monitoring methods.

Method	Device	Contactless	No diaper modification	Insensitive to visual occlusion
[2], [11], [5], [8]	Indicator line	✗	✓	✗
[6], [9], [4], [10]	Specific sensor	✗	✓	✓
[26], [32], [38], [25]	Specific RFID tag and reader	✓	✗	✓
[27]	Commercial RFID tag and reader	✓	✗	✓
Wet-Ra	Radar	✓	✓	✓

wetness monitoring, customized sensors, e.g., temperature monitoring [22], Geecare [6], Opro9 [9], Diapersens [4], and PIPI [10], have been designed to detect diaper wetness and send the results to smartphones via Bluetooth. Nonetheless, these sensors need to be manually adhered to diapers and removed from the wet diaper to be re-attached to a new diaper during a diaper change, which is relatively cumbersome for users. RFID tags have also been used for diaper wetness detection [25–27, 32, 38], but an RFID reader is needed to read the results within a certain distance.

In stark contrast to existing diaper wetness methods, in this paper, we explore the possibility of using RF signals to realize contactless, ubiquitous, and continuous diaper wetness monitoring. We aim to infer the wetness condition of diapers from radio signals that exhibit distinct patterns when reflected by dry or wet diapers. The system does not require any modifications to diapers. Thus, *Wet-Ra* is applicable to all off-the-shelf diapers. No visual checking or sensor displacement is needed, making the system convenient and user-friendly. Table 1 shows a comparison of different diaper wetness detection approaches.

However, to materialize the idea of an RF-based diaper wetness monitoring system, we are facing the following challenges.

- *How to extract informative representations from RF signals that embody the wetness conditions of diapers?*

Although there are many existing works on RF-based human activity detection, as far as we know, there is no precedent RF-based diaper wetness detection approach. It is difficult to extract fine-grained signal representations that contain sufficient details to help differentiate wet diapers from dry diapers.

- *How to eliminate multi-path interference that degrades the quality of signal representations?*

The indoor environment has a rich set of stationary and mobile objects that will reflect RF signals. The multi-path interference will distort the signal representations and affect the final detection accuracy.

- *How to establish a robust detection model that is applicable to new users in new environments?*

Learning-based models suffer from performance degradation when the training data distribution differs from that of test data, limiting the application of the detection model to new users and new environments.

We address the above challenges in our design of *Wet-Ra*, an RF-based diaper wetness detection system that utilizes commercial radar devices. *Wet-Ra* features three key components, i.e., Continuous-Radio-Snapshot (CRS) representation refinement, signal profile extraction, and transferable model construction. In the first step of CRS representation refinement, we compute Continuous-Radio-Snapshot based on the reflected Frequency Modulated Continuous Wave (FMCW) signals. To remove multi-path interference from the CRS, we leverage the background noise elimination method, subtracting the background CRS from the raw CRS. In the second step of signal profile extraction, we leverage wavelet multisynchrosqueezing transform [18] to derive clear and smooth signal profiles from the CRS without the smearing effects. In the last step of transferable model construction, we design a

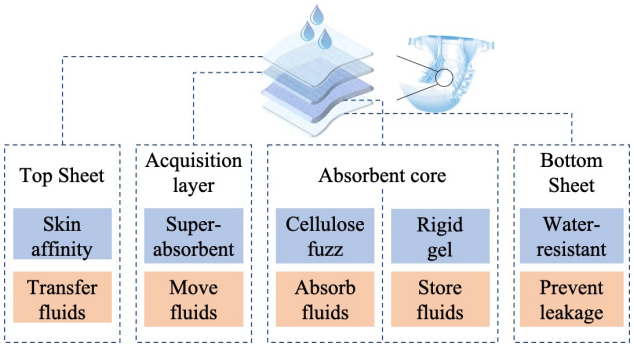

Fig. 1. The components of commodity diapers.

Heuristic Domain Adaptation network [16] architecture with a carefully-designed training dataset segmentation strategy. We conduct extensive experiments with 47 volunteers in 7 different rooms using three different brands of diapers. Experiment results verify that *Wet-Ra* can achieve a detection accuracy of more than 95%. We also demonstrate that *Wet-Ra* can adapt to a new user with less than 30 seconds of data from the new user. Therefore, *Wet-Ra* can be deployed in hospitals for inpatients care or nursing rooms for senile care. *Wet-Ra* can also be portable for a specific person at different places, e.g., transferred to a new hospital with a new environment.

We highlight our key contributions as follows.

- To the best of our knowledge, we make the first attempt to investigate the feasibility of diaper wetness detection using RF signals and realize a contactless, ubiquitous and convenient diaper wetness detection system *Wet-Ra*.
- We design a series of sophisticated algorithms to derive informative signal representations from the Continuous-Radio-Snapshot of RF signals and refine signal profiles by multi-path interference elimination.
- We develop a transferable wetness detection model adaptable to new users and new environments with high prediction accuracy.
- We implement and evaluate *Wet-Ra* in real-world settings with extensive experiments. The results demonstrate that *Wet-Ra* can detect diaper wetness with high accuracy.

2 PRELIMINARIES

In this section, we first present how to generate the Continuous-Radio-Snapshot (CRS) leveraging off-the-shelf mmWave Radars. Then, we demonstrate the captured CRS used for diaper wetness monitoring.

2.1 Diaper Absorption Mechanism

A diaper is an underwear that allows the user to urinate or defecate, which is widely used in various situations (e.g., babies and patients) [3]. As shown in Fig. 1, the typical diaper consists of four components.

- **Top sheet**. This layer is in contact with the skin. Its function is to transfer fluids while being soft and dry.
- **Acquisition layer**. This layer is under the top sheet. It consists of superabsorbent polymers, which absorb fluids many times their weight. Its function is to move the liquid from the top sheet to the next layer.
- **Absorbent core**. This layer is the core part of a diaper. It consists of cellulose fuzz and polyacrylate granules (rigid gel). The cellulose fuzz absorbs the liquid, and then the polyacrylate granules trap the liquid. Finally, the rigid gel turns soft and wobbly to keep the user's skin dry.

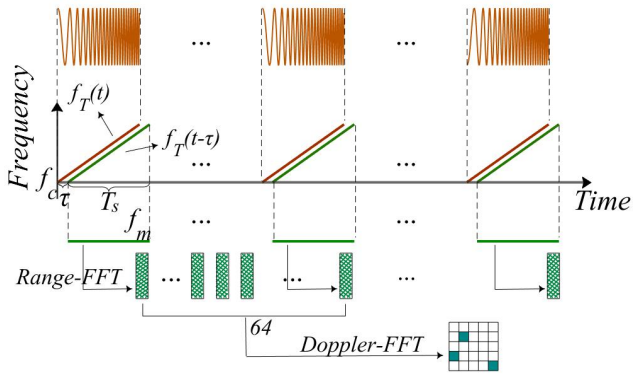

Fig. 2. Continuous-radio-snapshot (CRS) generation. The signal in the time domain is shown at the top. $f_T(t)$ is the transmitted signal. $f_T(t-\tau)$ is the reflected signal. f_m represents $S_{M1}(t)$ in Section 2.2. f_c is the start frequency. B is the sweep bandwidth. T_s is the sweep time. τ is the time delay of the reflected signal.

- **Bottom sheet**. This layer is a water-resistant outer layer of diapers. It allows the passage of water vapor and air to reduce moisture. Its function is to prevent liquid leakage.

2.2 Continuous-Radio-Snapshot

The biggest challenge of monitoring diaper wetness using commodity radars is how to extract informative features from radar signals that can be used to infer wetness levels. Most existing works used Frequency Modulated Continuous Wave (FMCW) of radars to detect distance and derive movements [21, 24, 37], which is not applicable to wetness detection. However, we have observed that dry and wet diapers' reflected radar signals exhibit distinct patterns. To characterize such differences, we derive Continuous-Radio-Snapshots from the received radar signals, which can be used to indicate different wetness levels.

As shown in Fig. 2, the frequency of the transmitted chirp signal increases linearly over time, denoted as $f_T(t) = f_c + \frac{B_s}{T_s}t$, where t is the time, f_c is the start frequency, B_s is the sweep bandwidth, and T_s is the sweep time. Accordingly, the phase of the transmitted chirp signal is $p(t) = \int_0^t f(t')dt' = 2\pi(f_c t + B_s\frac{t^2}{2T_s})$. The transmitted signal can be represented as

$$S_T(t) = cos\left(\int_0^t f(t')dt\right) = cos\left(2\pi(f_c t + \frac{B_s t^2}{2T_s})\right),$$

where $cos(\cdot)$ is the cosine function, and $\frac{B_s}{T_S}$ is the slope of the sweep. The amplitude of the sweep signal is assumed to be 1. The received signal is

$$S_R(t) = S_T(t-\tau) = cos\left(2\pi(f_c(t-\tau) + \frac{B_s(t-\tau)^2}{2T_s})\right),$$

where τ denotes the time delay of the reflected signal. The attenuation of the signal amplitude is ignored. Multiplying the received signal with the transmitted signal, we obtain $S_{M1}(t) = S_R(t) * S_T(t) = \frac{1}{2}(cos[2\pi(f_c t + \frac{B_s t^2}{2T_s}) + 2\pi(f_c(t-\tau) + \frac{B_s(t-\tau)^2}{2T_s})] + cos[2\pi(f_c t + \frac{B_s t^2}{2T_s}) - 2\pi(f_c(t-\tau) + \frac{B_s(t-\tau)^2}{2T_s})])$. Filtering the first high-frequency component, we can obtain

$$S_{M1}(t) = cos\left(2\pi(f_c\tau - \frac{B_s(\tau^2 - 2t\tau)}{2T_s})\right).$$

Fig. 3. Application scenario of *Wet-Ra*.

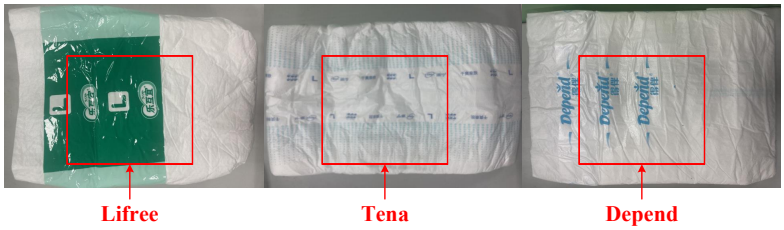

Fig. 4. Commodity diaper brands, i.e., Lifree, Tena, Depend.

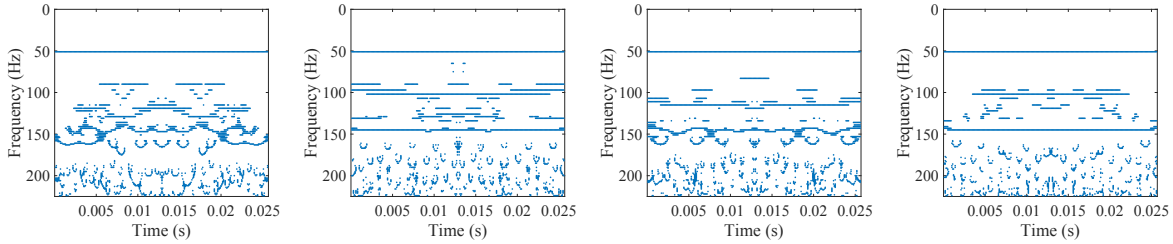

(a) Dry diaper, cotton trousers. (b) Wet diaper, cotton trousers. (c) Dry diaper, polyester trousers. (d) Wet diaper, polyester trousers.

Fig. 5. Signal profiles by WMSST of a specific user for wet and dry diapers when wearing different trousers. The data is collected in the basic setting in room A.

We apply range-FFT to $S_{M1}(t)$ to capture the detailed context of the reflected signal as $S_{M2}(t) = rangeFFT(S_{M1}(t))$. The duration of one chirp signal is α_t. We construct a Continuous-Radio-Snapshot (CRS) using a series of chirps as

$$CRS(t) = dopplerFFT(S_{M2}(t_1, t_2, ..., t_{64})),$$

where $S_{M2}(t_1, t_2, ..., t_{64})$ represents a time series of $S_{M2}(t)$. The time duration of one CRS is $\alpha_t * N$ms, where α_t is the duration of chirp.

2.3 CRS-Representation of Diaper Wetness

We visualize the CRS representations of radar signals reflected by wet and dry diapers. We collect data from 5 volunteers in room A, as shown in Fig. 3 and Fig. 17, using commodity diapers as shown in Fig. 4.

Fig. 5 demonstrates the signal profiles of a specific volunteer extracted based on CRS (the details of profile extraction in Section 3.3) from dry diapers and wet diapers when the wearing trousers made of different materials (cotton and polyester). We can observe that the signal profiles of dry diapers are similar no matter whether the user wears cotton or polyester trousers. However, the signal profiles of dry diapers are different from those of wet diapers, even if the user wears the same trousers. To quantify the similarity between signal profiles, we calculate the structural similarity index (SSIM) [30], which measures the structural differences between two images. A larger value of SSIM indicates a higher similarity between the two profiles. As shown in Table 2, the SSIM between the signal profiles of the same settings (wet/dry diaper, cotton/polyester trousers) is the highest. The SSIM between dry diapers and wet diapers is lower than between diapers of the same wetness level regardless

Table 2. SSIM of signal profiles by WMSST

SSIM	Dry, cotton	Dry, polyester	Wet, cotton	Wet, polyester
Dry, cotton	67.15%	65.97%	59.3%	62.67%
Dry, polyester	-	71.38%	60%	65.95%
Wet, cotton	-	-	74.95%	70.67%
Wet, polyester	-	-	-	75.74%

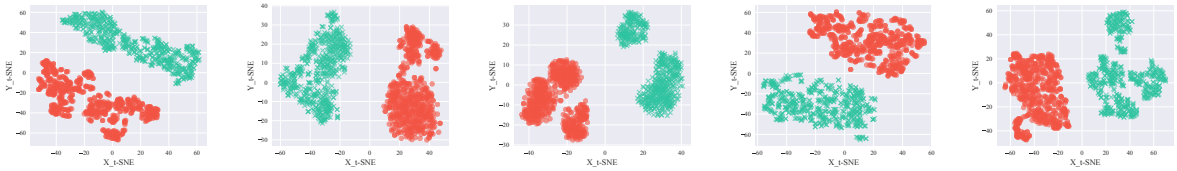

(a) User 1. (b) User 2. (c) User 3. (d) User 4. (e) User 5.

Fig. 6. The t-SNE value distribution of wet (red) and dry (green) diapers of different users in the basic scene. Note that each dot represents the t-SNE value of a signal profile collected in the scene.

of what trousers are worn. These results show the possibility of differentiating wetness levels of diapers based on the CRS of reflected radar signals.

We further apply t-distributed stochastic neighbor embedding (t-SNE) [29] to the signal profiles to visualize the distributions of signal profiles of wet and dry diapers of different users under different states. Fig. 6 shows the t-SNE value distributions of different users in the same scene (the basic scene in Table 4). Fig. 7 shows the t-SNE value distributions of wet and dry diapers of a single user in different scenes (angles, distances, and sleeping positions). We can observe that in both Fig. 6 and Fig. 7, t-SNE value distributions of wet and dry diapers are well separated. Note that the orientation of the point clouds in Fig. 6 and Fig. 7 is irrelevant as the t-SNE mainly focuses on separating different classes.

2.4 Challenges

To materialize a ubiquitous and contactless RF-based diaper wetness monitoring system, we are facing the following challenges.

- **Extracting informative representations.** Previous works have used RF signals for vital sign detection [37], temperature measurement [15], sleep posture monitoring [35], tire wear measurement [24], grid map construction [23], user identification [33], and medication self-administration monitoring [36]. Nonetheless, RF signals have never been leveraged for wetness detection. Specifically, the resolution of off-the-shelf radar devices is limited, making it difficult to derive fine-grained signal representations needed for wetness detection. To address this challenge, we refine Continuous-Radio-Snapshot (CRS) derived from RF signals, obtaining an informative representation that contains indicative features for wetness detection.
- textbfEliminating multi-path interference. In the indoor environment, RF signals will be reflected by multiple static and mobile objects (e.g., wall, ceiling, running fans), of which the interference will drown the information of diaper wetness. As a result, the received signal is a mixture of multi-path reflections entwined in a complicated non-linear manner. To tackle this problem, we develop a signal profile construction algorithm, which removes multi-path interference and extracts clear signal profiles for wetness detection.

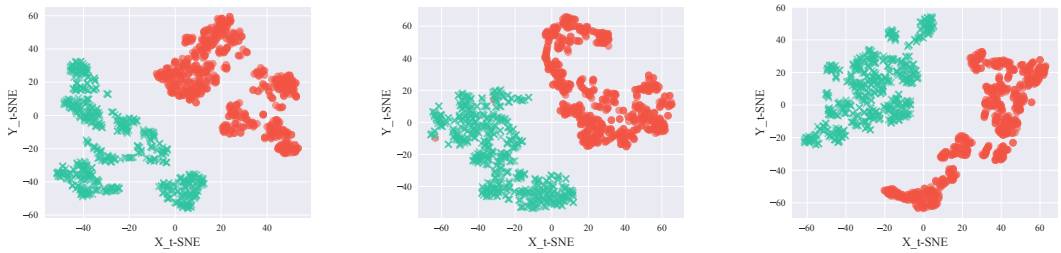

(a) Basic (b) Distance = 65cm. (c) Distance = 80cm.

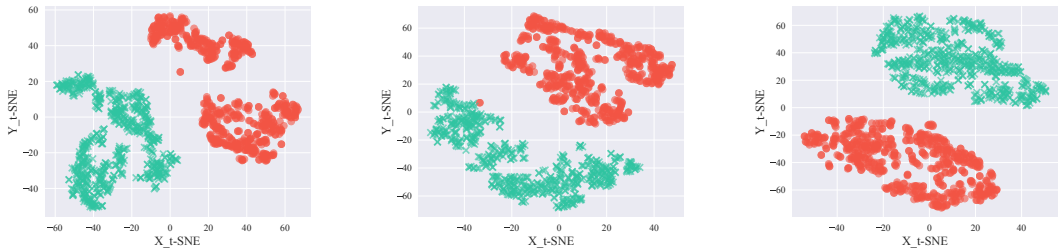

(d) Left side. (e) Right side. (f) Prone.

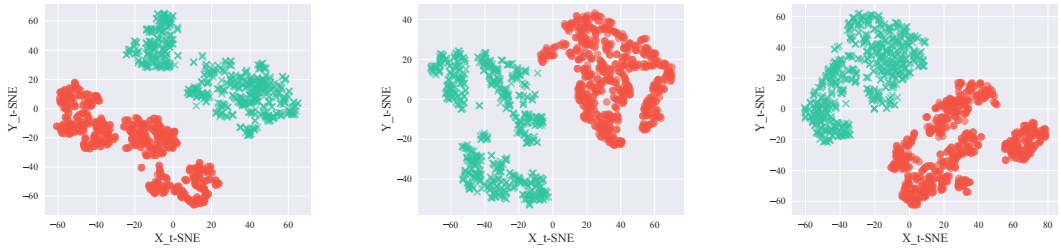

(g) Angle= 15°h. (h) Angle = 30°h. (i) Angle = 45°h.

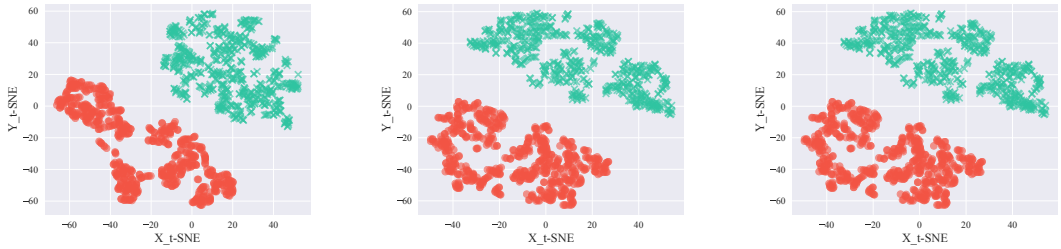

(j) Angle = 60°h. (k) Angle = 15°v. (l) Angle = 30°v.

Fig. 7. The t-SNE value distribution of wet (red) and dry (green) diapers of the same users in different scenes. Note that each dot represents the t-SNE value of a signal profile collected in the scene. The caption under each figure describes the setting that is different from the basic scene. °v and °h represent vertical and horizontal angles respectively.

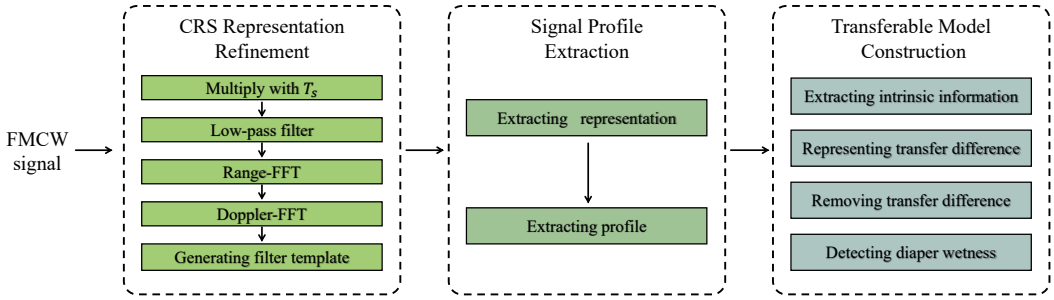

Fig. 8. Architecture of *Wet-Ra*.

- **Adapting to new persons in new environments.** Machine learning-based classification models are susceptible to the difference between training and test data. A well-performed model trained with the data of a specific person in a specific room will yield poor results when used by another person in another room. To extend the applicability of our system, we build a transferable model that can adapt to new users and new environments.

3 *WET-RA*: DETAILED CONSTRUCTION

3.1 Overview

As shown in Fig. 8, *Wet-Ra* mainly consists of three modules, i.e., CRS representation refinement, signal profile extraction, and transferable model construction.

- *CRS representation refinement.* We compute CRS that corresponds to the reflected signals by the diapers in the radar's field of view (FOV). To remove multi-path interference, we develop two filter templates and select the strongest component in the filtered CRS as the signal representation for wetness detection.
- *Signal profile extraction.* We derive the signal profile based on the refined CRS representation to extract representative features for wetness detection. In particular, we leverage wavelet multisynchrosqueezing transform to further eliminate the smearing artifact in signal representation and obtain a clear signal profile.
- *Transferable model construction.* We develop a transfer model that can predict diaper wetness for new users and new rooms. Firstly, we extract intrinsic information of samples from the source and the target domain. Secondly, we extract the difference in samples between the source domain and the target domain. Thirdly, since the data from the target domain do not have labels, we remove the transfer difference to identify the domain information for the extracted intrinsic information. Finally, the extracted information is used to detect diaper wetness.

3.2 Data Collection

As shown in Fig. 9, we utilize a commercial off-the-shelf (COTS) mmWave radar [7] to transmit and receive RF signals, and COTS DCA1000EVM [1] to stream out the sensing data to a computer via 1-Gbps Ethernet. The frequency range of the radar is 77Ghz ~ 81Ghz, so the wavelength of the transmitted signal is 4mm. The number of transmitting and receiving antennas is four and three, respectively. All antennas are co-located. The radar has a horizontal FOV of 120° and a vertical FOV of 30°. The slope of the FMCW chirp signals is set as 29.982Mhz/us, and each chirp contains 256 data samples. The sampling rate of ADC is 10, 000k/s. The radar board costs $299,

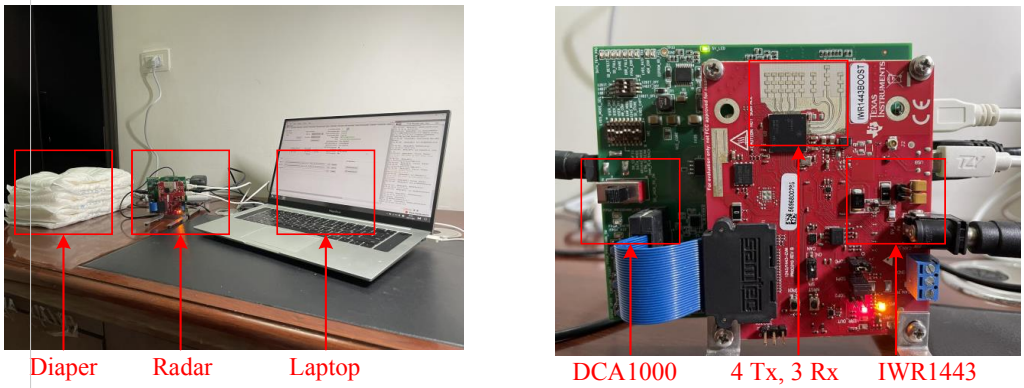

(a) The system of *Wet-Ra*.

(b) The radar composition.

Fig. 9. Experiment setup.

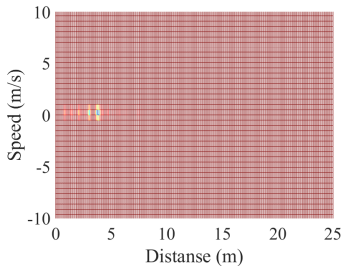

Fig. 10. The background CRS_0.

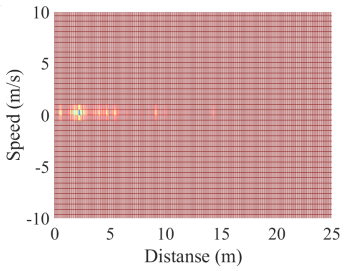

Fig. 11. The breathing reference CRS_b.

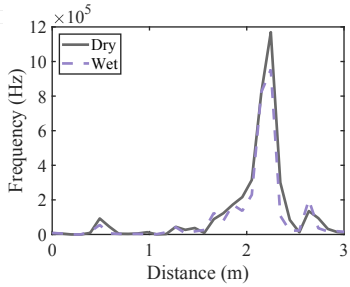

Fig. 12. Frequency-domain signal representations of wet and dry diapers.

and its core chip only costs $40. Unlike indicator lines or RFIDs, the system does not need to be discarded or replaced at every diaper change and can last long.

3.3 CRS Representation Refinement

The raw CRS computed according to Section 2.2 contains complicated multi-path interference. Therefore, we filter the interference in CRS, and then derive the signal representation from the refined CRS.

3.3.1 Filtering Multi-path Interference. As the multi-path interference is complicated and hard to model, we adopt the method of background noise elimination. More specifically, we build the CRS_0 when there is no user in the FOV of the radar, as shown in Fig. 10. We remove the background interference by

$$CRS' = CRS * CRS_0,$$

where CRS and CRS' are the raw CRS and the refined CRS, respectively. As shown in Fig. 13, the raw CRS contains sprawling highlighted components due to multi-path interference. After refinement, the CRS is more focused on the components that belong to the reflected signals of the diaper.

Since the diaper is worn on the body, the CSR is also affected by the user's breathing. To remove the influence of breathing, we collect a reference CRS when the user does not wear the diaper but the underwear. We normalize

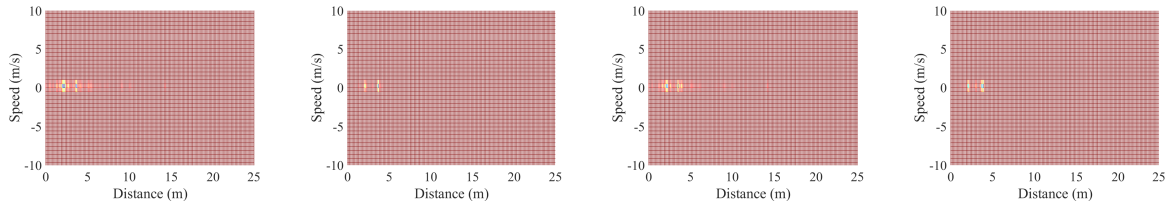

(a) Raw CRS (dry). (b) Refined CRS (dry). (c) Raw CRS (wet). (d) Refined CRS (wet).

Fig. 13. Filtering multi-path interference in the CRS.

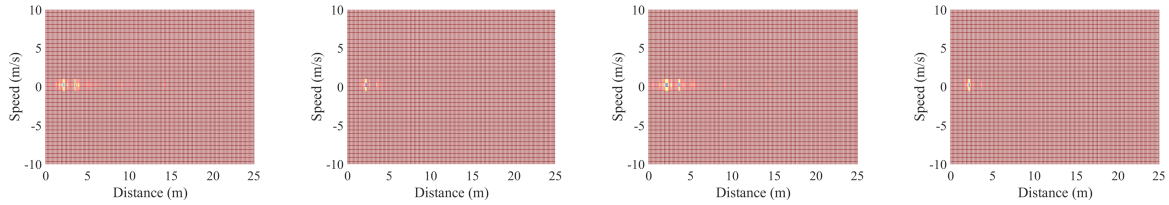

(a) Before breath removal (wet). (b) After breath removal (wet). (c) Before breath removal (dry). (d) After breath removal (dry).

Fig. 14. Filtering the interference of breathing in the CRS.

this CRS as CRS_b, as shown in Fig. 11. We filter the interference of breathing as

$$CRS'' = CRS' * CRS_b,$$

where CRS'' is the CRS after removing the interference of breathing. As shown in Fig. 14, the CRS after multi-path effect cancellation contains fake highlighted components due to breathing. After breathing removal, the CRS can eliminate the impact of breathing.

3.3.2 Extracting Signal Representations. After CRS refinement, we select the strongest component in the CRS and transform the strongest component by Inverse fast Fourier transform (IFFT) to obtain the signal representation as

$$S = \text{abs}(IFFT(CRS_{max})), \text{where } CRS_{max} = \max_{\Omega_i}(CRS''),$$

where Ω_i represents the serial set of points around the maximum value of CRS''. We set $i = 256$ empirically.

As shown in Fig. 12, the signal representations of the wet and the dry diapers have distinct patterns in the frequency domain. One of the main reasons is that the diaper's internal material will produce gels when meeting with water, and the gels in wet diapers will absorb part of the transmitted RF signals.

3.4 Signal Profile Extraction

Given the signal representation, we aim to extract the signal profile from the representation to capture the features of diapers of different wetness levels. Previous works used Continuous Wavelet Transform (CWT) [17] or wavelet synchrosqueezed transforms (WSST) [18] for signal profile extraction. Due to the Heisenberg uncertainty principle [14], these methods often generate vague time-frequency (TF) graphs of the representation. To address this problem, we apply wavelet multisynchrosqueezing transform (WMSST) [18] to obtain the signal profile.

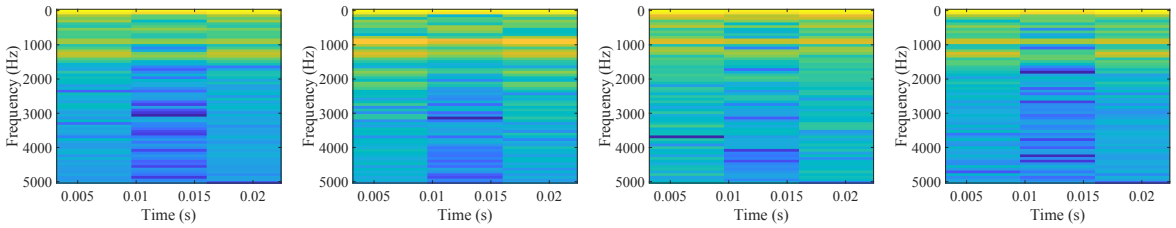

(a) Dry diaper, cotton trousers. (b) Wet diaper, cotton trousers. (c) Dry diaper, polyester trousers. (d) Wet diaper, polyester trousers.

Fig. 15. Signal profiles by STFT for wet and dry diapers when the user wears different trousers. The data is the same as in Fig. 5.

Table 3. SSIM of signal profiles by STFT

SSIM	Dry, cotton	Dry, polyester	Wet, cotton	Wet, polyester
Dry, cotton	61.01%	56.18%	64.8%	55.76%
Dry, polyester	-	62.68%	58.9%	64.52%
Wet, cotton	-	-	61.5%	60.35%
Wet, polyester	-	-	-	64.77%

WMSST utilizes a stepwise iterative reassignment to concentrate the vague TF graphs.

$$WMSST_f(\omega_b, \tau) = (\Delta\omega)^{-1} \sum_{a_k:A} W_f(a_k, \tau) a_k^{-\frac{3}{2}} (\Delta a)_k,$$

where $WMSST_f(\omega_b, \tau)$ is the transformed spectrum, ω_b is the center of bin $[\omega_b - \frac{1}{2}\Delta\omega, \omega_b + \frac{1}{2}\Delta\omega]$, τ is the resolution time domain, and a_k is the discrete value of the k-th scale. We have $(\Delta a)_k = a_k - a_{k-1}$, $\Delta\omega = \omega_b - \omega_{b-1}$, $A = |\omega(a_k, \tau) - \omega_b| \leq \frac{\Delta\omega}{2}$, and $W_f(a_k, \tau) = a_k^{-\frac{1}{2}} \int_{\mathbb{R}} S\psi(\frac{t-\tau}{a_k})dt$, where $\psi(\cdot)$ is a wavelet base function. We choose Morlet wavelet base function for its high resolution in both the frequency domain and the time domain. After computing $WMSST_f(\omega_b, \tau)$, we conduct multiple wavelet synchrosqueezing transform to refine the time-frequency representation as

$$P(\omega_l, \tau) = \int_{-\infty}^{+\infty} WMSST_f(\omega_b, \tau)\delta(\omega_l - \widetilde{\omega}_b^{[M]}(\omega_b, \tau))\mathrm{d}\omega_b,$$

where P is the signal profile, M is the number of wavelet synchrosqueezing transforms, ω is the instantaneous frequency, τ and ω_b are time and frequency, respectively, $\delta()$ is the Kronecker Dirac delta function, and $\widetilde{\omega}_b^{[M]}(\omega_b, \tau))$ is the instantaneous frequency estimate of $WMSST^{[M]}$ profiles. Since the number of wavelet synchrosqueezing transforms is uncertain, we limit the value of M utilizing a constraint condition

$$\int_{-\infty}^{+\infty} \int_{-\infty}^{+\infty} |\widetilde{\omega}_b^{[M]}(\omega_b, \tau) - \widetilde{\omega}_b^{[M-1]}(\omega_b, \tau)|\mathrm{d}\tau\mathrm{d}\omega_b < \epsilon,$$

where ϵ is a small threshold. We set ϵ as 10^{-8} empirically.

We utilize WMSST but not STFT because WMSST extracts fractal characteristics of wavelets, which enables wavelets to capture the local similarity of the input signals. According to Eq. 2.2, CRS consists of a series of chirps,

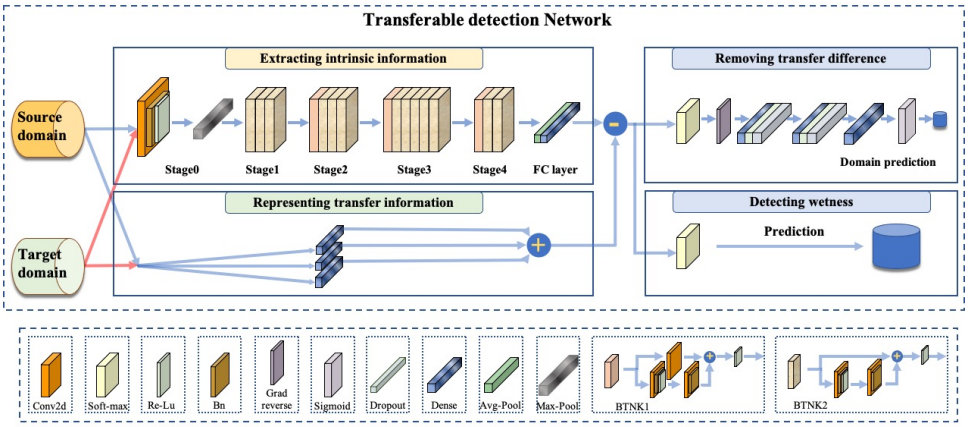

Fig. 16. Transferable model architecture.

and the chirp signals reflected by wet diapers may contain similar information. WMSST can condense and distill similar information for better detection.

To validate our choice, we compare the processed signal of WMSST and that of STFT. As shown in Fig. 15, the signal profiles extracted by STFT for wet and dry diapers do not show clear patterns. Moreover, as shown in Table 3, the SSIM of STFT signal profiles are indistinctive between wet and dry diapers, which confirms the superiority of WMSST over STFT in distinguishing signals of wet and dry diapers.

The time-frequency spectrum in Eq. 3.4 captures informative features of diapers of different wetness levels. As shown in Fig. 5(a) and Fig. 5(b), the signal profile of a dry diaper is conspicuously different from that of a wet diaper. Extracting a clear and distinct signal profile is essential for accurate prediction of diaper wetness.

3.5 Transferable Model Construction

When humans have learned from an example, e.g., a cat in a photo, he/she can recognize cats in many other different photos taken at different distances, angles, and backgrounds. The signal profile is used to train a classification model to learn about diaper wetness through RF sensing. We expect the trained model to be able to detect diaper wetness in different environments. However, conventional machine learning models suffer from significant performance degradation if the test data samples have a different distribution from the training data samples. To tackle this problem, we construct a transferable model that leverages the knowledge learned in the source domain with a few samples from the target domain to quickly adapt to new environments.

As shown in Fig. 16, the transferable model is based on Heuristic Domain Adaptation Network [16], which contains four phases: 1) extracting a feature representation from the signal profile, 2) computing the difference between the feature representations of the original and other scenes, 3) removing the difference, and 4) predicting the diaper wetness based on the features.

3.5.1 Extracting Intrinsic Information. It is difficult to manually decide which features are informative for wetness detection. Therefore, we utilize deep neural networks to extract feature presentations. More specifically, we adopt ResNet [20] to extract the feature representation $F(x_i)$, where x_i is the signal representation. We choose ResNet to extract the intrinsic information because the residual connection in ResNet can combine local information in low-layer networks and global information in deep-layer networks. In addition, the residual connection makes this sub-network more flexible in structure.

3.5.2 Representing Transfer Difference. To achieve stable prediction results, we need to eliminate the difference in the feature representation at different scenes. In other words, we need to distill intrinsic and general features that are essential for wetness detection and remove irrelevant information. Therefore, we establish a neural network to derive the transfer difference, denoted as $H(x_i)$, which converges to zero $H(x_i) \rightarrow 0$ as irrelevant information is gradually removed during training.

3.5.3 Removing Transfer Difference. To remove the transfer difference, we adopt the generative adversarial network (GAN). Specifically, we add a neural network after *Intrinsic Information Extraction* to form a GAN architecture. The GAN consists of a generator and a discriminator. The generator is used to extract the feature representation $F(x_i)$, where x_i is the signal representation, and the discriminator is used to identify whether the signal representation is from the source domain or the target domain. In addition, we add a Gradient Reversal Layer [19] in the discriminator to train the discriminator and the generator simultaneously.

The generator takes the signal representation from the source or the target domain as the input and outputs its feature presentation. The discriminator takes the feature presentation as the input and outputs the domain identification result. The loss function of the generator is $\mathcal{L}_G = -\mathbb{E}_{x_i^n \sim D_N} \log D(F_i)$, where F_i is the feature representation, x_i is the signal representation from the source domain, D is the discriminator, and D_N is the set of samples from the source domain. The loss function of the discriminator is $\mathcal{L}_D = \mathbb{E}_{x_i^n \sim D_N}(-\log D(F_i)) + \mathbb{E}_{x_j^a \sim D_A}(-\log[1 - D(F_j)])$, where F_j is the feature representation, x_j is the signal representation from the target domain, and D_A is the set of samples from the target domain. After training, the generator can generate a feature representation that embodies essential features for wetness detection under different scenes.

3.5.4 Detecting Wetness. We leverage a neural network to predict diaper wetness based on the feature representation after transfer difference removal. The loss function of the neural network is $L_P = \mathcal{L}_{CE}(F(x_i) - H(x_i), y_i)$, where y_i is the label of the sample (i.e., wet or dry), and $\mathcal{L}_{CE}$ is the cross-entropy of two variables.

3.5.5 Implementation. According to Fig. 16, we implement the intrinsic information extraction module using ResNet-34. The sub-network of transfer information representation is implemented by three parallel fully-connected layers with 2 neurons each. We implement the transfer difference removal module with two fully-connected layers with 1,024 neurons each, followed by a dropout layer (the drop rate is 0.5) and a LeakyRuLU layer as the activation function. After this, we add a fully-connected layer and use a Sigmoid function to output the domain information. Finally, the wetness detection result is produced by a softmax layer.

4 EVALUATION

We conduct extensive experiments to evaluate the performance of *Wet-Ra* to answer the following questions.

- **(Q1)** Is *Wet-Ra* capable of detecting diaper wetness with high accuracy?
- **(Q2)** Is the design of *Wet-Ra* contributive to the prediction accuracy?
- **(Q3)** Is *Wet-Ra* robust in different scenes?

4.1 Experiment Setup

We develop a fully functional prototype of *Wet-Ra* with a commercial off-the-shelf (COTS) radar [7] without any hardware or software modifications. The algorithms are implemented in Python 3 and Pytorch 1.5, and run on a MacBook with Intel Core i5 CPU at 2.4GHz and 8G memory running under macOS operating system, connected to the DCA1000EVM through an Ethernet cable.

We have recruited 47 participants (11 females and 36 males) aging from 18 to 34 with heights from 150cm to 186cm and weights from 41kg to 90kg. The experiments are conducted in seven different rooms. Three popular brands of diapers are evaluated, i.e., Depend [2], Tena [11], and Lifree [8]. The data collection expands from

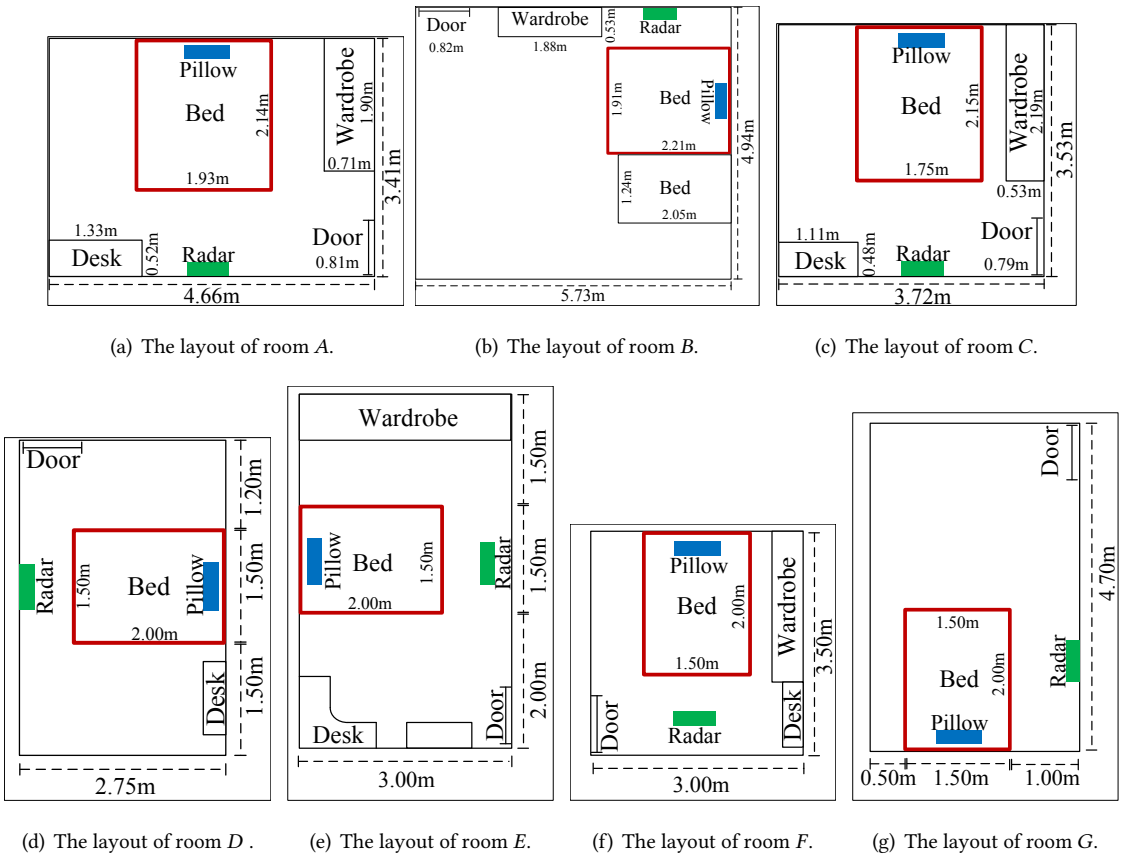

(a) The layout of room *A*. (b) The layout of room *B*. (c) The layout of room *C*.

(d) The layout of room *D* . (e) The layout of room *E*. (f) The layout of room *F*. (g) The layout of room *G*.

Fig. 17. Different environments for evaluations. The green square is the radar, and the blue square is the pillow.

March 7, 2021 to October 4, 2021. In total, we have collected over 787, 200 samples from the 47 participants for evaluation. The samples are labeled as positive (wet diapers) and negative (wet diapers). We simulate wet diapers by pouring 100ml of water on the diapers. We display all experiment scene setups in Table 4, in which "basic" is the default setting. In the default setting, we set the distance between the bed end and the radio device as 50cm, the horizontal and the vertical angles between the radio device and the diapers as 0°, and the user as lying supine. Our experiments are approved by the Ethics Committee of our university. Each user is compensated with $10 for participating in the experiments.

The evaluation metrics are defined as follows.

- Accuracy. Accuracy is the ratio of correctly identified samples to all samples.
- Precision. Precision is the ratio of correctly identified wet diapers to all identified wet diapers.
- Recall. Recall is the ratio of correctly identified wet diapers to all real wet diapers.
- F1-score. F1-score is a balance between precision and recall.
- False alarm rate (FAR). FAR is the probability of identifying dry diapers as wet diapers.
- Missing alarm rate (MAR). MAR is the probability of identifying wet diapers as dry diapers.

Table 4. Experiment setup for different scenes. (- represents basic setup.)

Setup	Distance	Angle horizontal	Angle vertical	Lying	Trousers	Brand	Breath	Room	People moving
Basic	50cm	0°	0°	Supine	-	-	-	-	w/o
35cm	35cm	0°	0°	Supine	-	-	-	-	w/o
65cm	65cm	0°	0°	Supine	-	-	-	-	w/o
80cm	80cm	0°	0°	Supine	-	-	-	-	w/o
15°h	50cm	15°	0°	Supine	-	-	-	-	w/o
30°h	50cm	30°	0°	Supine	-	-	-	-	w/o
45°h	50cm	45°	0°	Supine	-	-	-	-	w/o
60°h	50cm	60°	0°	Supine	-	-	-	-	w/o
15°v	50cm	0°	15°	Supine	-	-	-	-	w/o
30°v	50cm	0°	30°	Supine	-	-	-	-	w/o
Facing left	50cm	0°	0°	Facing left	-	-	-	-	w/o
Facing right	50cm	0°	0°	Facing right	-	-	-	-	w/o
Prone	50cm	0°	0°	Supine	-	-	-	-	w/o
Trousers	50cm	0°	0°	Supine	Five kinds (Sec. 4.5.4)	-	-	-	w/o
Brand	50cm	0°	0°	Supine	-	Lifree, Depend, Tena	-	-	w/o
Breath	50cm	0°	0°	Supine	-	-	Shallow, Deep	-	w/o
Room	50cm	0°	0°	Supine	-	-	-	Seven kinds (Fig. 17)	w/o
People moving	50cm	0°	0°	Supine	-	-	-	-	w/o, w

- Receiver operating characteristic (ROC) curve. ROC gauges the performance of a classifier under various discrimination thresholds.
- Equal error rate (EER). EER is the point where FAR equals FRR.
- Area under the curve (AUC). AUC is the ability of a classifier to distinguish between a wet diaper and a dry diaper.

4.2 Transferability

To evaluate the transferability of *Wet-Ra*, we evaluate three transfer scenarios. Note that the *basic* scene is shown in Table 4.

- **T1**. The source domain is the basic scene of a specific user, and the target domain is another scene of the same user.
- **T2**. The source domain is the basic scene of a specific user, and the target domain is all other scenes of the same user.
- **T3**. The source domain is the basic scene of a pair of two users, and the target domain is another scene of the same pair of users.

In each scenario, we train a model using 100% of labeled samples from the source domain and 30% of labeled samples from the target domain. The remaining 70% of target domain data samples are used for test.

For scenario **T1**, we evaluate the performance of *Wet-Ra* for the 47 users in different rooms and show the results in Table 5. It can be observed that *Wet-Ra* can achieve an average accuracy of 99.73% for wetness detection.

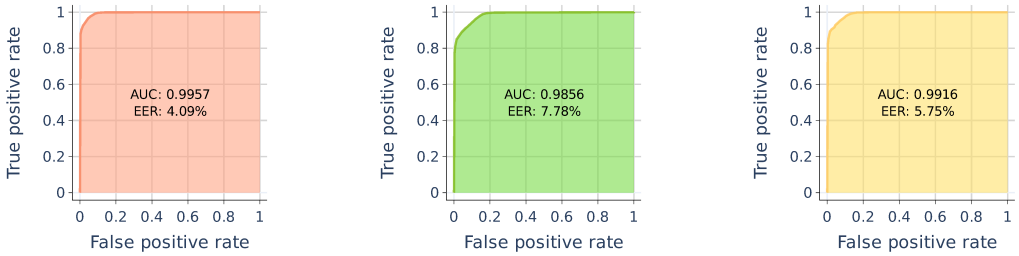

(a) Basic. (b) 15°v. (c) 15°h.

Fig. 18. ROC curve of *Wet-Ra* under different scenes.

We perform 1, 3, and 5-folds cross-validation on the B⇒B scenario. The average accuracy among the 47 users is 99.98%, 99.83%, and 99.82%, respectively, with a standard deviation of 0.0896. As shown in Fig. 18, the AUCs of *Wet-Ra* are 99.57%, 98.56%, and 99.16% when at the basic scene, the scene where the vertical angle is 15°, and the scene when the horizontal angle is 15°, respectively. Furthermore, the EERs are 4.09%, 7.78%, and 5.75% in the three scenes, respectively. These results demonstrate that *Wet-Ra* can accurately detect diaper wetness in real environment.

For scenario **T2**, we evaluate the performance of *Wet-Ra* for the 39 users in different rooms and show the results in Table 6. It can be observed that *Wet-Ra* can achieve an average accuracy of 98.81% for wetness detection. As shown in Fig. 19, Fig. 20 and Fig. 21, half of the participants have precision, recall, and F1-Score of higher than 99%. Furthermore, the false alarm rate and missing alarm rate of all participants are no more than 3%. These results demonstrate that *Wet-Ra* can adapt to different scenes utilizing the transferable detection model. We notice that, in our dataset, the average accuracy of male subjects is higher than that of female subjects. The possible reason is that males have a larger magnitude of chest movements due to breathing such that the change in radar signals is clearer. This enables us to build a more accurate CRS_b for filtering background interference.

For scenario **T3**, we evaluate the performance of *Wet-Ra* across different users in different rooms and show the results in Table 7. Specifically, there are four pairs, i.e., "User1-User2", "User3-User4", "User5-User6", "User7-User8". Moreover, the average accuracy of these pairs under all scenes is 99.64%, 97.2%, 99.67%, and 99.33%, respectively. The average accuracy of "User3-User4" under different scenes is 97.2%. The gender of these two users is different, which results in a vast difference in data distribution. We perform 1, 3, and 5-folds cross-validation on the B⟶B scenario. The average accuracy of these four pairs is 99.86%, 99.23%, 99.27%, and 99.74%, respectively, with a standard deviation of 0.3217. These results demonstrate that *Wet-Ra* can adapt to different users utilizing the transferable detection model.

We also analyze the detection time and the computation cost of *Wet-Ra*. The total detection time is no more than 0.7ms, and the computation cost is 81M. These show that *Wet-Ra* can monitor diaper wetness in a real-time manner.

4.3 Adaptability

We study whether *Wet-Ra* can quickly adapt to new users. For a specific user, we first train a detection model with all data of the other 46 users and then fine-tune the model with only 10% data (about 128 samples, less than 30 seconds) of the user himself/herself. The model is tested on the remaining 90% data of the user. Fig. 22 shows

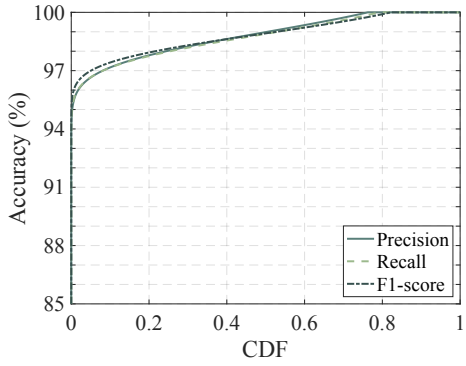

Fig. 19. The CDF of precision, recall, and F1-score of *Wet-Ra*.

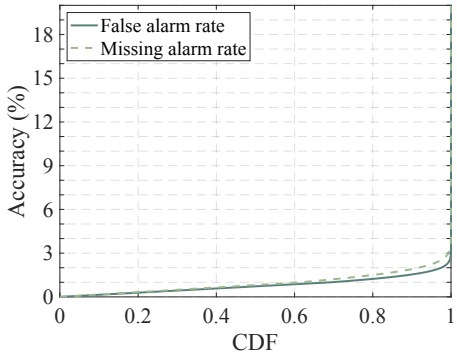

Fig. 20. The CDF of FAR and MAR of *Wet-Ra*.

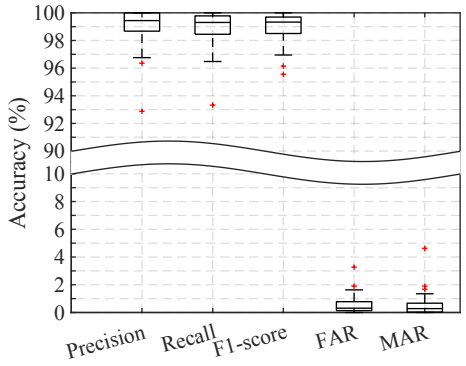

Fig. 21. The overall performance of *Wet-Ra*.

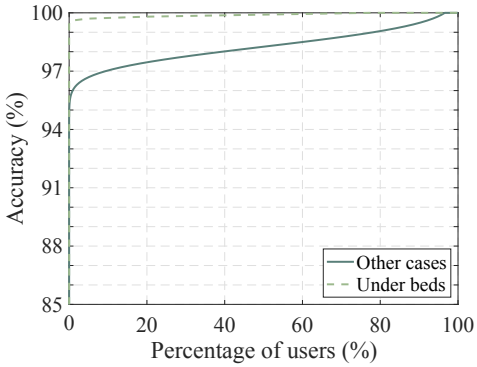

Fig. 22. The adaptability of *Wet-Ra*.

the CDF of detection accuracy of all 47 users. We can observe that more than 50% of the model has an accuracy of more than 97%. The average accuracy is 98.26%. This validates that *Wet-Ra* can quickly adapt to a new user by fine-tuning a pre-trained generalizable model on a few samples from the new user.

4.4 Ablation Study

We evaluate the effectiveness of the two design modules of *Wet-Ra*, i.e., CRS representation refinement and transferable model construction.

4.4.1 CRS Representation Refinement. We evaluate the performance of *Wet-Ra* under different numbers of chirps for CRS. When the number of chirps is set as 32, 64, 128, 225 in Equ. (2.2), the detection accuracy is 99.44%, 100.00%, 100.00%, and 99.66%, respectively. When the number of chirps is small, e.g., 64, the accuracy increases with more chirps. *Wet-Ra* has the highest accuracy when the number of chirps is 64 and 128. However, if the number of chirps further increases, the accuracy in turn decreases. One of the possible reasons is that as the number of chirps is large, the number of out-of-order packets also increases. We found that when the number of chirps is 64, the average out-of-order packet index is 3, but the average out-of-order packet index increases to 16 when the number of chirps is 225.

Table 5. The performance of *Wet-Ra* in transfer scenario **T1**. The left/right side of "→" is the source/target domain. The trained model is evaluated by the test data of the target domain. "-" represents null. "B": basic. "FL": facing left. "FR": facing right. "FD": prone.

Users	B→35cm	B→B	B→65cm	B→80cm	B→ 15°h	B→ 30°h	B→ 45°h	B→ 60°h	B→ 15°v	B→ 30°v	B→FL	B→FR	B→FD
User1	98.44%	100.00%	98.10%	100.00%	100.00%	98.55%	98.66%	100.00%	99.42%	98.76%	100.00%	98.70%	100.00%
User2	98.85%	100.00%	100.00%	96.85%	100.00%	100.00%	97.90%	99.16%	99.79%	100.00%	99.81%	100.00%	98.74%
User3	100.00%	100.00%	100.00%	87.50%	100.00%	99.77%	100.00%	99.67%	100.00%	99.89%	100.00%	99.67%	100.00%
User4	100.00%	100.00%	100.00%	100.00%	99.55%	99.78%	100.00%	100.00%	99.78%	99.55%	99.89%	100.00%	99.89%
User5	100.00%	100.00%	100.00%	99.89%	100.00%	100.00%	100.00%	100.00%	100.00%	100.00%	100.00%	100.00%	100.00%
User6	93.53%	100.00%	100.00%	96.76%	99.67%	99.55%	99.67%	98.99%	99.44%	98.33%	99.00%	99.78%	99.89%
User7	100.00%	100.00%	100.00%	100.00%	98.66%	99.78%	100.00%	100.00%	100.00%	95.53%	100.00%	99.44%	100.00%
User8	100.00%	100.00%	100.00%	100.00%	100.00%	100.00%	100.00%	100.00%	100.00%	100.00%	100.00%	100.00%	100.00%
User9	99.67%	100.00%	100.00%	97.88%	99.78%	100%	100.00%	100.00%	99.11%	100.00%	99.78%	99.67%	97.66%
User10	100.00%	100.00%	100.00%	100.00%	100.00%	99.89%	100.00%	99.89%	100.00%	100.00%	100.00%	100.00%	100.00%
User11	100.00%	100.00%	100.00%	100.00%	-	-	-	-	-	-	100.00%	100.00%	100.00%
User12	100.00%	100.00%	100.00%	100.00%	100.00%	100.00%	99.78%	100.00%	100.00%	100.00%	100.00%	100.00%	100.00%
User13	100.00%	100.00%	100.00%	100.00%	100.00%	100.00%	99.78%	100.00%	100.00%	100.00%	100.00%	100.00%	100.00%
User14	100.00%	100.00%	100.00%	100.00%	-	-	-	-	-	-	100.00%	100.00%	100.00%
User15	100.00%	100.00%	100.00%	100.00%	-	-	-	-	-	-	100.00%	100.00%	100.00%
User16	-	100.00%	-	-	-	-	-	-	100.00%	100.00%	100.00%	100.00%	100.00%
User17	98.33%	100.00%	100.00%	99.89%	-	-	-	-	-	-	-	-	-
User18	-	100.00%	-	-	100.00%	100.00%	100.00%	100.00%	-	-	100.00%	100.00%	100.00%
User19	99.78%	99.89%	100.00%	100.00%	100.00%	100.00%	99.89%	100.00%	100.00%	100.00%	100.00%	99.89%	100.00%
User20	99.44%	100.00%	99.89%	100.00%	-	-	-	-	-	-	100.00%	99.55%	99.89%
User21	99.78%	100.00%	100.00%	99.78%	-	-	-	-	99.55%	100.00%	99.67%	100.00%	99.89%
User22	100.00%	100.00%	100.00%	100.00%	100.00%	100.00%	100.00%	100.00%	99.89%	100.00%	100.00%	99.33%	100.00%
User23	99.55%	100.00%	99.55%	100.00%	-	-	-	-	99.78%	100.00%	100.00%	100.00%	97.77%
User24	97.55%	100.00%	99.89%	99.44%	-	-	-	-	99.55%	99.78%	100.00%	100.00%	99.78%
User25	99.89%	100.00%	98.88%	99.67%	100.00%	100.00%	99.33%	100.00%	100.00%	100.00%	100.00%	100.00%	100.00%
User26	100.00%	100.00%	99.78%	99.89%	98.00%	98.44%	98.66%	99.67%	99.78%	98.44%	-	-	-
User27	99.67%	100.00%	100.00%	100.00%	-	-	-	-	99.44%	100.00%	100.00%	99.89%	98.77%
User28	99.78%	100.00%	100.00%	100.00%	-	-	-	-	-	-	100.00%	100.00%	100.00%
User29	100.00%	100.00%	100.00%	100.00%	100.00%	100.00%	99.89%	99.78%	100.00%	100.00%	100.00%	100.00%	100.00%
User30	100.00%	100.00%	100.00%	100.00%	99.55%	99.44%	99.89%	100.00%	99.67%	100.00%	99.89%	100.00%	99.78%
User31	100.00%	100.00%	99.78%	99.89%	100.00%	100.00%	99.11%	100.00%	99.78%	100.00%	100.00%	100.00%	100.00%
User32	99.67%	100.00%	99.67%	99.78%	97.32%	98.77%	99.55%	99.22%	100.00%	99.44%	99.44%	98.00%	100.00%
User33	100.00%	100.00%	100.00%	100.00%	100.00%	100.00%	100.00%	99.89%	100.00%	100.00%	100.00%	99.78%	99.89%
User34	100.00%	100.00%	100.00%	100.00%	99.78%	99.00%	99.33%	99.33%	100.00%	99.00%	100.00%	100.00%	99.44%
User35	99.33%	100.00%	99.89%	100.00%	98.44%	99.55%	99.11%	99.78%	100.00%	98.88%	100.00%	100.00%	99.89%
User36	100.00%	100.00%	100.00%	100.00%	100.00%	99.78%	100.00%	100.00%	98.66%	99.67%	99.00%	98.33%	100.00%
User37	100.00%	100.00%	100.00%	100.00%	-	-	-	-	99.78%	100.00%	99.78%	99.89%	99.78%
User38	100.00%	100.00%	99.67%	100.00%	99.67%	98.55%	100.00%	99.11%	99.55%	99.78%	100.00%	99.89%	100.00%
User39	100.00%	100.00%	100.00%	100.00%	100.00%	100.00%	99.78%	100.00%	99.00%	99.55%	100.00%	100.00%	100.00%
User40	100.00%	100.00%	99.33%	99.89%	99.78%	100.00%	100.00%	100.00%	100.00%	99.89%	99.89%	100.00%	100.00%
User41	100.00%	100.00%	100.00%	100.00%	100.00%	100.00%	100.00%	100.00%	100.00%	100.00%	100.00%	100.00%	100.00%
User42	100.00%	100.00%	100.00%	100.00%	100.00%	100.00%	100.00%	100.00%	100.00%	100.00%	-	-	-
User43	99.44%	99.11%	99.11%	99.78%	-	-	-	-	99.44%	99.89%	99.33%	99.44%	99.89%
User44	100.00%	100.00%	99.89%	99.67%	100.00%	99.00%	99.67%	100.00%	100.00%	100.00%	99.89%	100.00%	100.00%
User45	-	100.00%	-	-	-	-	-	-	-	-	100.00%	100.00%	100.00%
User46	-	100.00%	-	-	-	-	-	-	-	-	100.00%	99.89%	100.00%
User47	-	100.00%	-	-	-	-	-	-	-	-	98.00%	99.22%	99.33%
Mean	99.58%	99.98%	99.84%	99.43%	99.67%	99.66%	99.67%	99.82%	99.76%	99.62%	99.85%	99.78%	99.77%

4.4.2 Transferable Model Construction. We compare the performance of using our proposed transferable model and a convolutional neural network (CNN). We randomly select 5 users. We train a ResNet-34 network for each user using all data samples at his/her basic scene. Then, we test the performance of the trained model under different scenes, as shown in Table 8. It is shown that the non-transferable detection model has lower accuracy and stability.

4.5 Robustness

4.5.1 Impact of Distances. We demonstrate that *Wet-Ra* is robust at different distances between the bed end and the radio device, i.e., 35cm, 50cm, 65cm, and 80cm. For each distance, we select 41 participants for data collection. Fig. 23 shows that *Wet-Ra* can achieve high accuracy in diaper wetness detection under different distances. The average accuracy is 98.59%, 100%, 99.71%, and 99.54% for each distance. The detection accuracy is inversely proportional to the distance. This is because the RF signal will attenuate as the distance between the bed end and

Table 6. The performance of *Wet-Ra* in transfer scenario **T2**. The left/right side of "→" is the source/target domain. The trained model is evaluated by the test data of a specific scene in (·). "-" represents null. "B": basic. "All": all scenes other than basic. "FL": facing left. "FR": facing right. "FD": prone.

Users	B→ All (35cm)	B→All (B)	B→All (65cm)	B→All (80cm)	B→All (15°h)	B→All (30°h)	B→All (45°h)	B→All (60°h)	B→All (15°v)	B→All (30°v)	B→All (FL)	B→All (FR)	B→All (FD)
User1	98.88%	100.00%	99.22%	99.11%	95.42%	97.32%	97.88%	99.33%	98.10%	97.32%	99.67%	98.44%	96.21%
User2	96.22%	100.00%	98.85%	98.53%	89.92%	99.58%	97.69%	96.43%	99.37%	99.27%	99.67%	98.42%	97.27%
User3	99.55%	100%	99.89%	100.00%	100.00%	100.00%	99.89%	100.00%	100.00%	98.33%	100.00%	100.00%	99.67%
User4	99.89%	100.00%	100.00%	100.00%	98.88%	99.89%	99.78%	99.89%	99.67%	99.78%	99.89%	99.67%	99.42%
User5	99.89%	100.00%	99.67%	99.55%	100.00%	100.00%	99.89%	99.78%	100.00%	98.10%	99.78%	98.77%	100.00%
User6	98.10%	100.00%	100.00%	98.66%	99.00%	99.11%	99.89%	100.00%	98.10%	99.55%	99.67%	99.33%	94.98%
User7	99.67%	99.67%	97.10%	96.21%	95.87%	98.33%	96.65%	98.10%	99.67%	95.87%	97.32%	97.43%	98.55%
User8	100.00%	100.00%	99.89%	99.67%	100.00%	100.00%	99.22%	98.77%	100.00%	99.44%	100.00%	99.67%	100.00%
User9	88.62%	99.89%	99.67%	97.21%	99.22%	98.77%	99.55%	99%	99.22%	98.66%	98.21%	98.21%	98.10%
User10	98.33%	99.89%	99.11%	99.78%	82.48%	91.97%	98.33%	97.55%	98.77%	99.78%	98.33%	98.44%	99.78%
User11	100.00%	100.00%	99.89%	100.00%	-	-	-	-	-	-	99.78%	100.00%	100.00%
User12	99.89%	100.00%	99.89%	99.67%	100.00%	100.00%	100.00%	99.11%	100.00%	100.00%	99.89%	99.22%	99.67%
User13	98.66%	100.00%	99.55%	96.09%	-	-	-	-	-	-	99.78%	97.88%	100.00%
User14	97.77%	99.88%	92.19%	90.85%	-	-	-	-	-	-	95.54%	98.33%	98.21%
User15	-	100.00%	-	-	-	-	-	-	100.00%	99.89%	99.00%	97.32%	99.55%
User16	98.33%	100.00%	100.00%	99.78%	-	-	-	-	-	-	-	-	-
User17	-	100.00%	-	-	99.78%	99.11%	99.33%	99.89%	-	-	97.66%	99.89%	97.77%
User18	98.33%	100.00%	100.00%	99.89%	99.67%	99.67%	99.78%	97.77%	99.55%	88.06%	100.00%	100.00%	99.33%
User19	98.55%	100.00%	99.00%	98.66%	-	-	-	-	-	-	99.33%	99.55%	99.55%
User20	99.22%	100.00%	100.00%	99.78%	-	-	-	-	98.88%	100.00%	98.66%	99.78%	99.33%
User21	94.09%	100.00%	99.55%	97.32%	98.88%	97.32%	99.89%	95.98%	97.77%	98.44%	97.32%	99.33%	99.00%
User22	98.10%	100.00%	98.00%	98.66%	-	-	-	-	95.88%	99.00%	98.88%	99.89%	95.65%
User23	97.88%	100.00%	99.78%	99.33%	-	-	-	-	98.88%	98.00%	99.11%	99.33%	99.33%
User24	99.11%	100.00%	98.00%	99.44%	100.00%	99.89%	97.10%	99.22%	99.78%	98.77%	99.89%	99.67%	99.67%
User25	100.00%	100.00%	98.55%	99.78%	97.32%	96.32%	98.44%	99.22%	97.66%	99.55%	-	-	-
User26	98.77%	99.44%	99.00%	99.55%	-	-	-	-	95.98%	99.11%	99.89%	99.67%	98.33%
User27	99.55%	99.89%	100.00%	99.67%	-	-	-	-	-	-	100.00%	100.00%	99.89%
User28	99.22%	100.00%	99.22%	99.89%	97.77%	99.89%	99.11%	97.32%	99.44%	99.78%	98.66%	98.77%	96.65%
User29	99.55%	100.00%	99.78%	99.55%	98.44%	99.67%	99.33%	99.78%	99.33%	99.67%	100.00%	97.88%	98.77%
User30	99.55%	100.00%	99.55%	99.67%	99.89%	99.89%	99.33%	99.89%	99.44%	99.78%	99.44%	99.78%	99.67%
User31	98.88%	100.00%	99.00%	99.00%	97.55%	98.10%	99.00%	98.33%	99.33%	99.44%	99.55%	95.65%	100.00%
User32	99.67%	100.00%	99.67%	99.78%	99.11%	99.33%	97.55%	98.10%	99.89%	99.67%	100.00%	99.89%	97.43%
User33	100.00%	100.00%	99.00%	99.89%	99.44%	98.33%	96.09%	99.11%	99.11%	98.21%	99.78%	99.11%	97.10%
User34	99.44%	100.00%	99.89%	100.00%	97.77%	98.00%	99.55%	99.89%	99.44%	98.88%	100.00%	99.11%	99.55%
User35	94.75%	99.78%	95.09%	99.11%	100.00%	99.11%	99.89%	99.89%	95.09%	97.66%	99.00%	94.64%	99.78%
User36	97.21%	100.00%	94.42%	99.89%	-	-	-	-	96.65%	98.77%	98.21%	99.22%	99.33%
User37	99.55%	100.00%	99.55%	99.67%	99.89%	99.44%	100.00%	98.33%	99.22%	98.10%	99.89%	99.55%	99.55%
User38	96.65%	100.00%	98.66%	99.11%	-	-	-	-	97.10%	97.21%	98.10%	97.55%	99.55%
User39	98.66%	100.00%	95.87%	98.66%	99.67%	96.88%	96.88%	99.67%	99.67%	99.33%	97.77%	98.55%	98.55%
Mean	98.39%	99.96%	98.82%	98.96%	97.92%	98.69%	98.85%	98.87%	98.78%	98.54%	99.13%	98.86%	98.79%

Table 7. The performance of *Wet-Ra* in transfer scenario **T3**. The left/right side of "→" is the source/target domain of the pair of users. The trained model is evaluated by the test data of the target domain of one of the pair of users. "B": basic. "FL": facing left. "FR": facing right. "FD": prone.

Users		B→35cm	B→B	B→65cm	B→80cm	B→ 15°h	B→ 30°h	B→ 45°h	B→ 60°h	B→ 15°v	B→ 30°v	B→FL	B→FR	B→FD
Pair1	User1	99.42%	99.55%	99.77%	100.00%	99.89%	99.55%	99.44%	99.89%	100.00%	99.42%	100.00%	98.33%	99.78%
	User2	100.00%	100.00%	100.00%	100.00%	99.00%	99.78%	100.00%	100.00%	99.44%	100.00%	99.89%	98.10%	99.44%
Pair2	User3	92.41%	100.00%	98.21%	97.43%	99.11%	93.42%	98.00%	93.00%	95.00%	97.21%	98.00%	99.67%	98.66%
	User4	86.05%	99.67%	98.88%	97.88%	98.55%	98.66%	99.11%	96.77%	98.88%	96.42%	98.10%	99.44%	98.66%
Pair3	User5	99.89%	99.78%	100.00%	99.44%	100.00%	100.00%	99.78%	99.78%	100.00%	99.11%	100.00%	99.78%	100.00%
	User6	99.55%	99.55%	99.89%	99.78%	99.44%	99.78%	99.89%	99.33%	99.89%	99.89%	97.88%	99.11%	100.00%
Pair4	User7	98.66%	100.00%	99.00%	99.89%	98.43%	100.00%	99.22%	97.32%	99.67%	99.00%	98.88%	98.33%	96.43%
	User8	100.00%	100.00%	100.00%	100%	99.00%	100.00%	99.89%	99.89%	100.00%	100.00%	100.00%	99.67%	99.22%

the radio device increases. Interestingly, the average accuracy is the lowest when the distance is 35cm. This is because the transferable detection model is trained on the data of scenes all with longer distances than 35cm.the

4.5.2 Impact of Angles. We show the robustness of *Wet-Ra* with different angles between the diapers and radio device, i.e., vertical angle 0°, vertical angle 15°, vertical angle 30°, horizontal angle 0°, horizontal angle 15°, horizontal angle 30°, horizontal angle 45°, and horizontal angle 60°. For each angle, we select 30 participants

Table 8. The performance of *Wet-Ra* without the transfer model. The non-transferable model is trained by all data samples of the basic scene and evaluated by the test data of a specific scene in (·). "B": basic. "FL": facing left. "FR": facing right. "FD": prone.

Users	(B)	(35cm)	(65cm)	(80cm)	(15°h)	(30°h)	(45°h)	(60°h)	(15°v)	(30°v)	(FL)	(FR)	(FD)
User1	100%	54.43%	18.23%	0.52%	56%	45.57%	91.93%	56%	100%	92.97%	92.19%	55.47%	50.52%
User2	100%	41.15%	64.58%	57.81%	66.15%	72.66%	77.08%	82.29%	30.73%	72.66%	85.42%	56.51%	60.94%
User3	100%	11.46%	45.83%	45.57%	71.62%	17.19%	10.41%	47.14%	53.13%	52.34%	52.08%	66.41%	48.70%
User4	100%	16.68%	84.64%	27.08%	93.22%	58.07%	36.46%	33.33%	46.35%	63.80%	36.46%	58.33%	89.84%
User5	100%	51.04%	48.70%	75.00%	100.00%	50.26%	49.74%	49.48%	50.26%	51.35%	25.78%	81.77%	50.00%

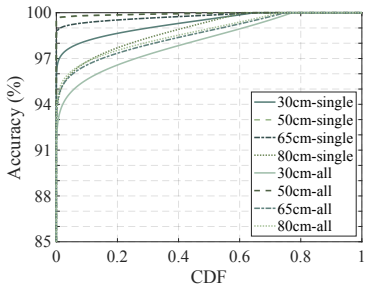

Fig. 23. Impact of distances.

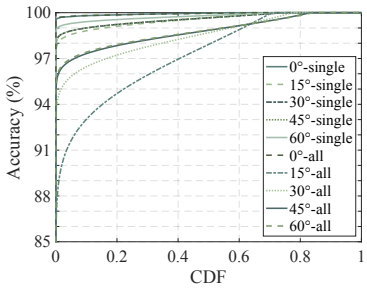

Fig. 24. Impact of horizontal angles.

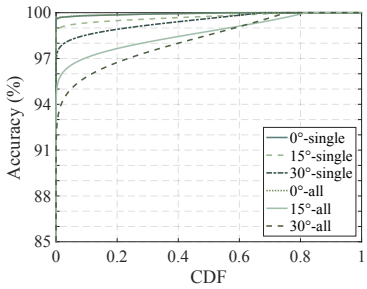

Fig. 25. Impact of vertical angles.

for data collection. Fig. 24 shows that the performance of *Wet-Ra* decreases with increased horizontal angles. *Wet-Ra* has the highest average accuracy when the horizontal angle is 0° since the RF signals are occluded less in this angle than at all other angles. According to Fig. 25, 60% of the samples have a detection accuracy of more than 99% in all vertical angles. The performance of *Wet-Ra* decreases with increasing vertical angles for similar reasons.

4.5.3 Impact of Room Sizes. We show that *Wet-Ra* is robust when the room has different sizes, i.e., 4.66m*3.41m, 5.73m*4.94m, 3.72m*3.53m, 3m*5m, 3m*3.5m, 3m*4.7m, and 2.75m*4.2m, as shown in Fig. 17. For each room, we select 2 participants for data collection. As shown in Fig. 26, the average accuracy of the basic scene is 98.84%, 99.77%, 99%, 99.81%, 100%, 99.64%, and 98.68% for each room, respectively. The average accuracy when the device is mounted at the wall is 99.77%, 99.77%, 99.94%, 99.89%, 99.33%, 100%, and 99.42% for each room, respectively. Different rooms have different attenuation and multi-path effects. However, the detection accuracy of *Wet-Ra* is over 98.68% in general.

4.5.4 Impact of Trousers. We show that *Wet-Ra* is robust when the user wears trousers made of different fabrics, including Dacron, cotton, flax, nylon, and CVC. We collect data from 3 participants wearing different trousers. Fig. 27 shows that the accuracy of diaper wetness detection is 100% for each fabric. When the diaper is wet, the hydrogel will become soft, wobbly, and conductive, significantly attenuating the RF signals. Since trousers made of these fabrics do not attenuate or absorb RF signals, *Wet-Ra* can achieve high accuracy of diaper wetness detection when the user wears trousers made of different fabrics.

4.5.5 Impact of Diaper Brands. We show that *Wet-Ra* is robust with different brands of diapers including Depend [2], Tena [11], and Lifree [8]. For each brand, we select 10 participants for data collection. Fig. 28 shows that Tena has the best performance. The average accuracy is the same for all diaper brands as they all have a similar structure. These results indicate that *Wet-Ra* is robust to the brand of diapers.

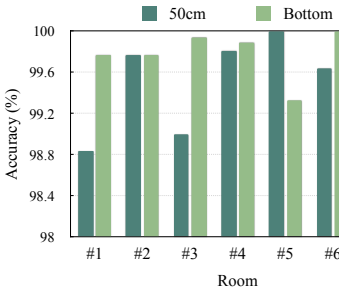

Fig. 26. Impact of rooms

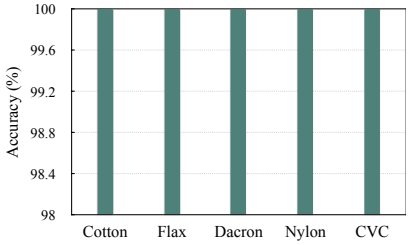

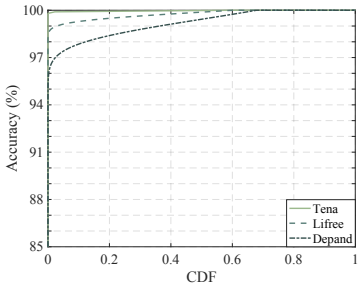

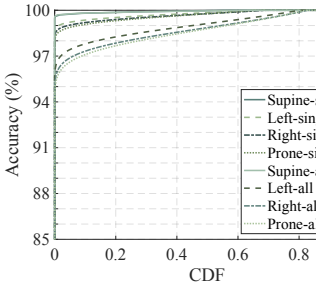

Fig. 29. Impact of lying post

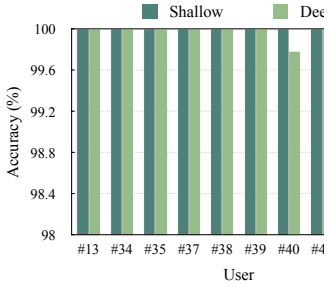

Fig. 30. Impact of breath inte

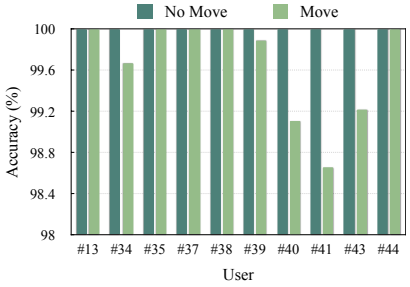

Fig. 31. Impact of moving people.

4.5.6 Impact of Lying Postures. We evaluate the performance of *Wet-Ra* with different lying postures of the participants, including supine, prone, left side, and right side. For each distance, we select 43 participants for data collection. As shown in Fig. 29, the accuracy of "-single" (scenario **T1**) is higher than "-all" (scenario **T2**). This is because more transfer difference has to be removed in scenario **T2**. According to Fig. 29, 60% of the samples have a detection accuracy of more than 99% in all postures. It is clear that the supine posture has the highest average accuracy and the postures facing left/right have similar average accuracy. This is because the supine posture has the best angle of view, and the facing left/right posture has a similar view angle. When the user's posture is prone, the radar signal will be partly covered by the human body, decreasing the average accuracy of this posture. The average accuracy of different postures is over 99.52%, which shows that *Wet-Ra* is robust to the lying postures.

4.5.7 Impact of Breath Intensity. *Wet-Ra* is robust when the user has a shallow or a deep breath. For each kind of breath, we select 10 participants for data collection. As shown in Fig. 30, the average accuracy is 100% and 99.97% for a shallow and a deep breath, respectively. We perform 1, 3, and 5-folds cross-validation on the deep breath scenario. The average accuracy among the ten users is 99.98%, 99.84%, and 99.90%, respectively, with a standard deviation of 0.0702. Although intensive respiration is good for locating diapers, the reflected RF signals will contain the noise introduced by abdominal motion when the user deliberately takes a deep breath. Therefore, the average accuracy of diaper wetness detection of deep breathing is lower than that of shallow breathing.

4.5.8 Impact of Moving People. We demonstrate the robustness of *Wet-Ra* when other people are moving in the room. We select 10 participants to lie in bed with 1 people moving around the bed. Fig. 31 shows that the average accuracy drops to 99.68% with people moving while the accuracy is 100% without people moving. We perform 1, 3, and 5-folds cross-validation on the scenario with one person moving around the bed. The average accuracy

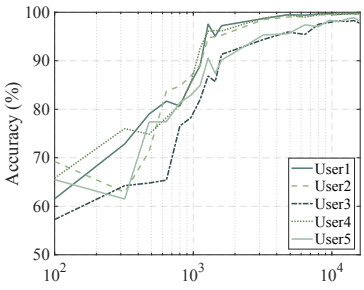

Fig. 32. Impact of training dataset size.

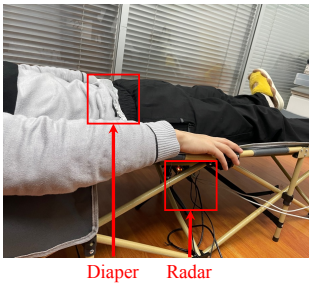

Fig. 33. Placing radar under be

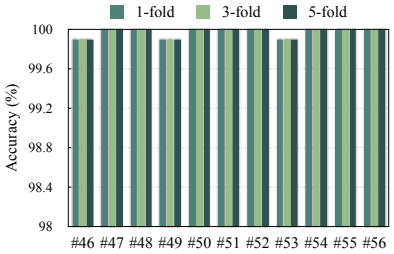

Fig. 34. Impact of under-bed radar placement.

among the ten users is 99.66%, 99.39%, and 99.30%, respectively, with a standard deviation of 0.1873. Since we use the user's breath to locate diapers, the movements of other people will interfere with the process of locating diapers. Specifically, a moving person will introduce new reflection paths.

4.5.9 Impact of Training Set Size. Since we adopt the transferable detection model, the size of the training dataset has a significant influence on the system performance. Fig. 32 shows the relationship between the training dataset size and the detection accuracy. With a larger training dataset, the accuracy of *Wet-Ra* increases quickly when the training dataset size is less than 1.6k. After the training dataset size reaches 4k, the accuracy does not increase much with more training samples.

4.5.10 Impact of Under-bed Radar Placement. We show the robustness of *Wet-Ra* when placing the radar under beds. As shown in Fig. 33, the radar is placed under the bed about 23cm away from the bed boards. A user is lying supine on the bed with diapers of Depend [2]. We collect data from 11 volunteers aged from 18 to 28 with a total of 21, 120 samples. As shown in Fig. 34, *Wet-Ra* achieves an average accuracy of more than 99% under all cross-validation scenarios, which demonstrates that *Wet-Ra* works well under the bed. We evaluate the adaptability of *Wet-Ra* when placing the radar under the bed. Fig. 22 shows that *Wet-Ra* achieves an average accuracy of 99.91%, which is higher than the case of placing the radar beside the bed. The possible reason is that when placing the radar under beds, the multi-path effect mainly comes from the bed and the user, while the multi-path effect of placing the radar beside the bed is more complicated, affected by all the objects in the room.

5 RELATED WORK

5.1 Special Sensor Based Diaper Wetness Detection

The majority of off-the-shelf diapers, such as Depend [2], Tena [11], Elderjoy [5], and Lifree [8], use a color-changing wetness indicator line to detect and exhibit the wetness level. However, the indicator line needs to be interwoven in every diaper and is obsolete when the diaper is discarded. Moreover, the indicator line cannot be easily checked when covered by trousers. To overcome this problem, customized sensors such as temperature monitoring [22], Geecare [6], Opro9 [9], Diapersens [4], and PIPI [10] have been developed to detect diaper wetness, which can send wetness detection results to smartphones through Bluetooth. A wearable gadget is designed to detect urination by sensing the outer surface of the diaper's temperature [22]. Geecare [6], Opro9 [9], Diapersens [4], and PIPI [10] are commercial off-the-shelf sensors. However, these sensors need to adhere to the diapers and re-attached to a new diaper for every diaper change, which is inconvenient and cannot be applied to common diapers.

5.2 RFID Based Diapers Wetness Detection

RFID have been leveraged [25–27, 32, 38] for monitoring diaper wetness. RFID tags are either customized [25, 26, 32, 38] or commodity RFID tags [27]. An RFID tag is placed in every diaper for one-time use. An expensive RFID reader (i.e., hundreds of dollars) is needed to scan and read the information from RFID tags. Sidén et al. [26] proposed a semi-passive high-frequency (HF) RFID tag for wetness detection that can be read by the RFID reader within 30cm. A passive but expensive HF RFID tag is designed in [32, 38], which can be read within 30cm. Pankhuri et al. [25] proposed an ultra-high frequency (UHF) RFID moisture monitor tag based on hydrogel sensing, which re-purposes diaper materials of Super Absorbent Polymer to detect moisture. Tanaka et al. [28] developed a self-powered sensor that is activated by urine, but the time delay of the system is long (5 minutes) due to the complex signal processing algorithm. Wei et al. [27] proposed to use commodity passive RFID tags for wetness detection but required a pair of tags on a diaper and needed one-time calibration to eliminate the tag-tag coupling effect before using.

5.3 RF Based Application

Recent years have witnessed vast development of RF-based applications, including human-related [12, 13, 33–37] and non-human-related sensing [15, 21, 23, 24, 31]. V2iFi [37] detects driver vital signs condition using a radio device installed at the windshield. Zhao et al. [36] proposed a contactless system to monitor medication self-administration. BodyCompass [35] utilized an FMCW radio device to monitor the sleep posture of users. MU-ID [33] utilized mmWave to identify users based on gaits. mmVib [21] captures micrometer-level vibrations utilizing a mmWave radar. ThermoWave [15] monitored temperatures through mmWave signals. mSens [31] used a commodity mmWave networking device to identify different materials. milliMap [23] leveraged a radar to reconstruct a dense grid map. Osprey [24] measured tire wear by a mmWave radar.

Different from all existing applications, *Wet-Ra* realizes diaper wetness monitoring using RF signals. We carefully derive the signal representation and extract the signal profile from the reflected signals that indicate the wetness level of a diaper. Moreover, we develop a transferable model that expands the usage of *Wet-Ra* to new users and new environments. Compared with existing diaper wetness monitoring systems, *Wet-Ra* is contactless, ubiquitous, and user-friendly.

6 LIMITATIONS AND FUTURE WORK

We have developed a primitive prototype of *Wet-Ra* that can perform data collection, signal processing, and wetness detection in a relatively ideal setting. To make *Wet-Ra* a viable product in the market, we still need to address various practical issues.

Independent-user system. We have shown that *Wet-Ra* can adapt to a new user with a few samples from the new user. However, if there is no data on the new user, the pre-trained model on all other users has an accuracy of lower than 60%. It is ideal but extremely difficult to make *Wet-Ra* entirely user-independent. There are three possible future directions to achieve this goal.

- *Hardware*. More advanced radar devices with more fine-grained signals will greatly enhance the detection performance.
- *Representation learning*. Another solution is to extract better representations of wetness/dryness from radar signals. Currently, individual differences greatly affect the detection accuracy of *Wet-Ra*. With more advanced representation learning techniques, we expect to extract user-independent features that only relate to the wetness of diapers.
- *Meta-learning*. Meta-learning is a fast-growing technique to extend the knowledge learned from one task to another. In the future, meta-learning may be utilized to improve the generality of *Wet-Ra*. For instance, data from similar tasks may be collected to strengthen the detection capability of *Wet-Ra*.

System setup requirements. During the data collection process, we filter multi-path interference from CRS by collecting two background references CRS_0 and CRS_b, which adds extra overhead when deploying *Wet-Ra* in a different environment for a different user. One possible solution is to parameterize CRS_0 and CRS_b for similar environments and similar users. For example, two hospital rooms with similar settings may have similar CRS_0 that depends on their size and furnishing. Two female users of similar physiological conditions may have similar CRS_b.

System integration. In our experiment, we collected data using the radar and ran the algorithm of wetness detection offline on computers. In the future, it is ideal for integrating *Wet-Ra* into a single and portable device that can be plugged into work conveniently. To achieve this goal, the detection model is better embedded into the device rather than in the cloud. In this way, the running of *Wet-Ra* will not require an internet connection, and the privacy of user data can be protected.

Complicated scenarios. We have evaluated the normal user position with one pair of trousers. There may be more complicated scenarios that will affect the performance of *Wet-Ra*.

- *User position*. If the user crosses their legs on the bed, the radar signal may be blocked, making it difficult to obtain the signal reflected from the diaper.
- *Trousers thickness*. If the user wears several layers of trousers or a relatively thick pair of trousers, the radar signal may not be able to penetrate the trousers to reach the diaper. The trousers may also have company/brand tags and metallic zip that may clutter the radar signal.
- *Diaper material*. The permeability, permittivity, and conductance of the diaper material will affect the RF signal transmission, which will affect the performance of wetness detection.
- *Body movement*. If the user performs large movements on the bed, the radar signal may be interfered. A possible solution is to track gradual average temporal changes due to wetness seepage rather than instant signal changes due to large body movement.

In the future, we aim to design more sophisticated algorithms to deal with more complicated scenarios and conduct more in-depth studies on the impact of diaper materials on RF signal loss.

7 CONCLUSION

In this paper, we introduce *Wet-Ra*, a contactless, ubiquitous, and user-friendly diaper wetness monitoring system based on RF signals. *Wet-Ra* works by extracting informative features for wetness detection from RF signals. Specifically, we design a series of sophisticated algorithms to derive informative signal representations from the Continuous-Radio-Snapshot (CRS) of RF signals and refine signal profiles by multi-path interference elimination. Then, a transferable wetness detection model adaptable to new users and environments is utilized to detect diaper wetness. Finally, we empirically evaluate *Wet-Ra* with 47 volunteers in 7 different rooms with three off-the-shelf diaper brands. Our results show that *Wet-Ra* can accurately identify diaper wetness in the real environment.

ACKNOWLEDGMENTS

We thank the anonymous reviewers for their constructive comments. Yanjiao's research is supported by the National Natural Science Foundation of China under Grant 61972296. Yanjiao Chen is the corresponding author.

REFERENCES

[1] 2021. DCA1000EVM. https://www.ti.com/tool/DCA1000EVM.
[2] 2021. Depend Incontinence Protection with Tabs, Maximum Absorbency, L, 48 Count (3 Packs of 16 Count) (Packaging May Vary). https://www.amazon.com/Depend-Incontinence-Protection-Maximum-Absorbency/dp/B01LTI00PQ/ref=sr_1_3?dchild=1&keywords=Depend+diapers&qid=1625024636&sr=8-3.
[3] 2021. Diaper. https://en.wikipedia.org/wiki/Diaper.

[4] 2021. DiaperSens Adult Incontinence Smart Diaper Sensor for Wet Diaper Alert. https://www.amazon.com/DiaperSens-Adult-Incontinence-Diaper-Sensor/dp/B07DBH8KXK/ref=cm_cr_arp_d_bdcrb_top?ie=UTF8.

[5] 2021. ELDERJOY ADULT DIAPER (L). https://shop.banitore.com.hk/en/collections/elderjoy/products/201?variant=35100442067099.

[6] 2021. Geecare Thin Smart Baby Wet Diaper Alarm Monitoring Baby Urine Regularity and Lost Prevent with Mobile Phone APP. https://www.amazon.com/Geecare-Diaper-Monitoring-Regularity-Prevent/dp/B06XTQW33B/ref=cm_cr_arp_d_bdcrb_top?ie=UTF8.

[7] 2021. IWR1443BOOST. https://www.ti.com/tool/IWR1443BOOST.

[8] 2021. Lifree Tape Stop Diaper Extendable Fit Thin Type Safe and Light Tape Stop L size 18 sheets 4 times absorption (for those who often spend time sleeping). https://www.amazon.com/Lifree-Diaper-Extendable-absorption-sleeping/dp/B0759B4XPT/ref=sr_1_1?dchild=1&keywords=Lifree+diapers&qid=1625023335&sr=8-1.

[9] 2021. Opro9 Smart Wearable Humidity Sensor Instant Alert Prevent Baby Diaper. https://www.amazon.com/Wearable-Humidity-Sensor-Instant-Prevent/dp/B01N8RD32C.

[10] 2021. PIPI Senior Wet Diaper Monitor. https://www.amazon.com/PIPI-Senior-Wet-Diaper-Monitor/dp/B084KXMSCM/ref=sr_1_1?dchild=1&keywords=Wet+Diaper+monitor&qid=1625021550&sr=8-1.

[11] 2021. Tena ProSkin Unisex Incontinence Adult Diapers, Maximum Absorbency, Extra Large, 48 ct. https://www.amazon.com/Incontinence-Briefs-Uni-Sex-Absorbency-XLarge/dp/B07RWVT51M/ref=sr_1_2?dchild=1&keywords=Tena+diapers&qid=1625023288&sr=8-2.

[12] Fadel Adib, Hongzi Mao, Zachary Kabelac, Dina Katabi, and Robert C Miller. 2015. Smart homes that monitor breathing and heart rate. In *Proceedings of the 33rd annual ACM conference on human factors in computing systems*. 837–846.

[13] Adeel Ahmad, June Chul Roh, Dan Wang, and Aish Dubey. 2018. Vital signs monitoring of multiple people using a FMCW millimeter-wave sensor. In *2018 IEEE Radar Conference (RadarConf18)*. IEEE, 1450–1455.

[14] Paul Busch, Teiko Heinonen, and Pekka Lahti. 2007. Heisenberg's uncertainty principle. *Physics Reports* 452, 6 (2007), 155–176.

[15] Baicheng Chen, Huining Li, Zhengxiong Li, Xingyu Chen, Chenhan Xu, and Wenyao Xu. 2020. ThermoWave: a new paradigm of wireless passive temperature monitoring via mmWave sensing. In *Proceedings of the 26th Annual International Conference on Mobile Computing and Networking*. 1–14.

[16] Shuhao Cui, Xuan Jin, Shuhui Wang, Yuan He, and Qingming Huang. 2020. Heuristic domain adaptation. *arXiv preprint arXiv:2011.14540* (2020).

[17] Ingrid Daubechies. 2009. *The wavelet transform, time-frequency localization and signal analysis*. Princeton University Press.

[18] Ingrid Daubechies, Jianfeng Lu, and Hau-Tieng Wu. 2011. Synchrosqueezed wavelet transforms: An empirical mode decomposition-like tool. *Applied and computational harmonic analysis* 30, 2 (2011), 243–261.

[19] Yaroslav Ganin and Victor Lempitsky. 2015. Unsupervised domain adaptation by backpropagation. In *International conference on machine learning*. PMLR, 1180–1189.

[20] Kaiming He, Xiangyu Zhang, Shaoqing Ren, and Jian Sun. 2016. Deep residual learning for image recognition. In *Proceedings of the IEEE conference on computer vision and pattern recognition*. 770–778.

[21] Chengkun Jiang, Junchen Guo, Yuan He, Meng Jin, Shuai Li, and Yunhao Liu. 2020. mmVib: micrometer-level vibration measurement with mmwave radar. In *Proceedings of the 26th Annual International Conference on Mobile Computing and Networking*. 1–13.

[22] Tareq Khan. 2018. A smart wearable gadget for noninvasive detection and notification of diaper moister. In *IEEE International Conference on Electro/Information Technology (EIT)*.

[23] Chris Xiaoxuan Lu, Stefano Rosa, Peijun Zhao, Bing Wang, Changhao Chen, John A Stankovic, Niki Trigoni, and Andrew Markham. 2020. See through smoke: robust indoor mapping with low-cost mmwave radar. In *Proceedings of the 18th International Conference on Mobile Systems, Applications, and Services*. 14–27.

[24] Akarsh Prabhakara, Vaibhav Singh, Swarun Kumar, and Anthony Rowe. 2020. Osprey: a mmWave approach to tire wear sensing. In *Proceedings of the 18th International Conference on Mobile Systems, Applications, and Services*. 28–41.

[25] Pankhuri Sen, Sai Nithin R Kantareddy, Rahul Bhattacharyya, Sanjay Emani Sarma, and Joshua E Siegel. 2019. Low-cost diaper wetness detection using hydrogel-based RFID tags. *IEEE Sensors Journal* 20, 6 (2019), 3293–3302.

[26] Johan Sidén, Andrei Koptioug, and Mikael Gulliksson. 2004. The" smart" diaper moisture detection system. In *IEEE MTT-S International Microwave Symposium Digest (IEEE Cat. No. 04CH37535)*.

[27] Wei Sun and Kannan Srinivasan. 2021. Healthy diapering with passive RFIDs for diaper wetness sensing and urine pH identification. In *International Conference on Mobile Systems, Applications, and Services*.

[28] Ami Tanaka, Ryota Suematsu, Hiroya Sakamoto, and Takakuni Douseki. 2016. Self-powered wireless urinary-incontinence sensor determines time for diaper change from spacing between sensing signals. In *2016 IEEE SENSORS*. IEEE, 1–3.

[29] Laurens Van der Maaten and Geoffrey Hinton. 2008. Visualizing data using t-SNE. *Journal of machine learning research* 9, 11 (2008).

[30] Zhou Wang, Alan C Bovik, Hamid R Sheikh, and Eero P Simoncelli. 2004. Image quality assessment: from error visibility to structural similarity. *IEEE transactions on image processing* 13, 4 (2004), 600–612.

[31] Chenshu Wu, Feng Zhang, Beibei Wang, and KJ Ray Liu. 2020. msense: Towards mobile material sensing with a single millimeter-wave radio. *Proceedings of the ACM on Interactive, Mobile, Wearable and Ubiquitous Technologies* 4, 3 (2020), 1–20.

[32] Kenji Yamada, Nagakura Toshiaki, Ken Ishihara, Yuko Ohno, Atsue Ishii, Sachiko Shimizu, Tomoyuki Araki, Rie Takahashi, Hideya Takahashi, and Eiji Shimizu. 2010. Development of new type incontinence sensor using RFID tag. In *IEEE International Conference on Systems, Man and Cybernetics*.

[33] Xin Yang, Jian Liu, Yingying Chen, Xiaonan Guo, and Yucheng Xie. 2020. MU-ID: Multi-user identification through gaits using millimeter wave radios. In *IEEE INFOCOM 2020-IEEE Conference on Computer Communications*. IEEE, 2589–2598.

[34] Shichao Yue, Hao He, Hao Wang, Hariharan Rahul, and Dina Katabi. 2018. Extracting multi-person respiration from entangled rf signals. *Proceedings of the ACM on Interactive, Mobile, Wearable and Ubiquitous Technologies* 2, 2 (2018), 1–22.

[35] Shichao Yue, Yuzhe Yang, Hao Wang, Hariharan Rahul, and Dina Katabi. 2020. BodyCompass: Monitoring sleep posture with wireless signals. *Proceedings of the ACM on Interactive, Mobile, Wearable and Ubiquitous Technologies* 4, 2 (2020), 1–25.

[36] Mingmin Zhao, Kreshnik Hoti, Hao Wang, Aniruddh Raghu, and Dina Katabi. 2021. Assessment of medication self-administration using artificial intelligence. *Nature medicine* 27, 4 (2021), 727–735.

[37] Tianyue Zheng, Zhe Chen, Chao Cai, Jun Luo, and Xu Zhang. 2020. V2iFi: in-Vehicle Vital Sign Monitoring via Compact RF Sensing. *Proceedings of the ACM on Interactive, Mobile, Wearable and Ubiquitous Technologies* 4, 2 (2020), 1–27.

[38] Mohamed A Ziai and John C Batchelor. 2015. Smart radio-frequency identification tag for diaper moisture detection. *Healthcare technology letters* 2, 1 (2015), 18–21.